

**Detection of an unbroken phase of a non-Hermitian system via a Hermitian factorization surface**Leela Ganesh Chandra Lakkaraju  and Aditi Sen(De) *Quantum Information and Computation Group, Harish-Chandra Research Institute, HBNI, Chhatnag Road, Jhansi, Allahabad 211 019, India*

(Received 1 July 2021; revised 23 September 2021; accepted 15 October 2021; published 24 November 2021)

In the traditional quantum theory, one-dimensional quantum spin models possess a factorization surface where the ground states are fully separable and have vanishing bipartite as well as multipartite entanglement. We report that in the non-Hermitian counterpart of these models, these factorization surfaces either can predict the exceptional points where the unbroken-to-broken transition occurs or can guarantee the spectrum to be real, thereby suggesting a procedure to reveal the unbroken phase. We first analytically demonstrate it for the nearest-neighbor rotation-time- ( $\mathcal{RT}$ ) symmetric  $XY$  model with uniform and alternating transverse magnetic fields, referred to as the  $iATXY$  model. Exact diagonalization techniques are then employed to establish this fact for the  $\mathcal{RT}$ -symmetric  $XYZ$  model with short- and long-range interactions as well as for the long-range  $iATXY$  model. Moreover, we show that although the factorization surface prescribes the unbroken phase of the non-Hermitian model, the bipartite nearest-neighbor entanglement at the exceptional point is nonvanishing.

DOI: [10.1103/PhysRevA.104.052222](https://doi.org/10.1103/PhysRevA.104.052222)**I. INTRODUCTION**

Over the years, studying the phenomena and properties of one-dimensional short-range quantum spin models in the presence of magnetic fields has generated a lot of interest [1,2] since several such Hamiltonians can be mapped to spinless fermions [3] and hard-core bosons [4], thereby ensuring the analytical study of single-, two-, and multisite features. Moreover, they can be simulated in laboratories with physical substrates like ultracold atoms [5], nuclear magnetic resonances [6–8], and ion traps [9]. Apart from investigating phenomena like quantum phase transitions at zero temperature and the quantum dynamical transition in evolution, these systems have been shown to be potential candidates for designing quantum technologies [10–13]. Moreover, these models also possess a factorization surface or volume in the parameter space, [14–20] at which the ground state is doubly degenerate and is fully separable, having vanishing bipartite as well as multipartite entanglement [21].

On the other hand, the seminal paper by Bender and Boettcher [22] showed that a non-Hermitian Hamiltonian with both parity and time-reversal symmetries (together called  $\mathcal{PT}$  symmetry) can have a real energy spectrum, while the breaking of the symmetry leads to the complex eigenenergy. The phase transition from the symmetry-broken phase to an unbroken phase occurs at the exceptional point. These results have stimulated a significant amount of research to characterize non-Hermitian quantum theory, both theoretically and experimentally, especially in optics [23], cold atoms [24], and cavities [25,26]. In this respect, discrete systems like the tight-binding model and quantum spin systems, specifically, one-dimensional quantum  $XY$  models, turn out to be important platforms to verify the properties of the non-Hermitian Hamiltonian [27–35]. It was also noticed that instead of  $\mathcal{PT}$  symmetry, the linear rotation operator  $\mathcal{R}$ , which rotates each spin by a certain amount around a fixed axis, along with

the time reversal operator  $\mathcal{T}$  can prompt non-Hermiticity in quantum spin models [36]. Specifically, it was shown that the nearest-neighbor transverse  $XY$  model with an imaginary anisotropy parameter has  $\mathcal{RT}$  symmetry and undergoes a transition from the unbroken phase to a broken one which can again be detected via the existence of change in the spectrum from real to imaginary ones. In both non-Hermitian fermionic and bosonic systems [37], Berry curvature [38] and multipartite entanglement [39] are used to describe the broken-to-unbroken transitions.

In the current work, we first investigate the one-dimensional (1D)  $\mathcal{RT}$ -symmetric nearest-neighbor  $XY$  model in the presence of uniform and alternating magnetic fields [40], which we call the  $iATXY$  model. The Hermitian version of this model possesses a richer phase diagram than that of the transverse  $XY$  model. In particular, it has a paramagnetic II phase with a large amount of bipartite entanglement along with antiferromagnetic (ferromagnetic) and paramagnetic I phases [41,42]. Moreover, like the  $XY$  model, it can also be diagonalized by Jordan-Wigner, Fourier, and Bogoliubov transformations [1,36,43–45]. By employing similar transformations in the non-Hermitian case, we report that the exceptional points which divide the real and imaginary spectra can be inferred from the factorization surface of the corresponding Hermitian Hamiltonian. The finite-size exact diagonalization calculations also confirm this result, thereby motivating us to consider quantum spin models which cannot be solved analytically.

To establish the relation between the broken-to-unbroken transition of the non-Hermitian model and the factorization surface of the Hermitian counterpart, we study both the nearest-neighbor and long-range  $\mathcal{RT}$ -symmetric  $XYZ$  model and the  $iATXY$  model with long-range interactions. In all these systems, numerical simulations strongly suggest that the unbroken phase of the  $\mathcal{RT}$ -symmetric models can be identified by the corresponding Hermitian factorization surface.

Specifically, we find that the energy spectrum is real at and above the surface predicted via the factorization surface of the Hermitian Hamiltonian, thereby providing a sufficient condition for the reality of the spectrum. Interestingly, we observe that at the surface, the bipartite nearest-neighbor entanglement of the  $iATXY$  model is nonvanishing. At this point, we are tempted to conjecture that the tuning parameter of the  $\mathcal{RT}$ -symmetric Hamiltonian which leads to a real spectrum can be determined from the factorization surface of the corresponding Hermitian models. It is important for the following three reasons. (1) In both the Hermitian and non-Hermitian domains, there are quantum spin models for which the spectrum can be found only numerically, although the factorization surfaces are known from the different symmetry properties of the system [16]. (2) Finding where the spectrum is real is not an easy task, owing to the computational problems of diagonalizing non-Hermitian Hamiltonians, although we know that any physics that is observable and measurable needs to be done when the spectrum is real. Our method directly prescribes either an exceptional point for the nearest-neighbor model or parameters that correspond to the real spectrum, thereby simplifying the situation enormously. (3) Lastly, our results possibly show that the properties of the Hermitian system have the potential to diagnose the exceptional point of the non-Hermitian systems without computation.

This paper is organized as follows. In Sec. II, we discuss the way to diagonalize the pseudo-Hermitian  $ATXY$  model, and the broken-to-unbroken transition identified via the factorization surface of the corresponding Hermitian model is presented in Sec. III. In Sec. IV, we confirm that the exceptional point is predicted by the factorization surface by considering the nearest-neighbor  $\mathcal{RT}$ -symmetric  $XYZ$  model. In Sec. IV B, the procedure for detecting the unbroken phase in both the models with long-range interactions having  $\mathcal{RT}$  symmetry is provided. The behavior of bipartite entanglement and parity in the transition surface of the  $iATXY$  model are described in Sec. V, and we conclude in Sec. VI.

## II. PSEUDO-HERMITIAN $iATXY$ MODEL

Let us first consider the pseudo-Hermitian one-dimensional nearest-neighbor  $XY$  model with an imaginary anisotropy factor in the presence of a uniform and alternating transverse magnetic field. The Hamiltonian reads

$$\hat{H}_{iATXY} = \sum_{i=1}^N J \left[ \frac{1+i\gamma}{4} \sigma_i^x \sigma_{i+1}^x + \frac{1-i\gamma}{4} \sigma_i^y \sigma_{i+1}^y \right] + \frac{h_1 + (-1)^i h_2}{2} \sigma_i^z, \quad (1)$$

where  $J \neq 0$  is the coupling constant,  $\sigma^{x,y,z}$  are Pauli matrices,  $i\gamma$  is the imaginary anisotropy parameter, and  $h_1 - h_2$  and  $h_1 + h_2$  are the strengths of the magnetic fields on odd and even spins, respectively. We also assume a periodic boundary condition throughout the paper, i.e.,  $\sigma_{N+1} = \sigma_1$ . Like the  $XY$  model with uniform field [36], we will show that the non-Hermitian  $\hat{H}_{iATXY}$  with  $\mathcal{RT}$  symmetry has a real spectrum in the unbroken phase, while the complex eigenenergy is found in the broken phase. Here  $\mathcal{R}$  is the application of  $\frac{\pi}{2}$

rotation about the  $z$  axis, given by  $\mathcal{R} \equiv e^{[-i(\pi/4) \sum_{j=1}^N \sigma_j^z]}$ , and the time reversal  $\mathcal{T}$  is the complex conjugation in the case of finite-dimensional systems. The Hamiltonian is not individually invariant under either the  $\mathcal{R}$  or  $\mathcal{T}$  operator, but when they are combined, the Hamiltonian is invariant under  $\mathcal{RT}$ , i.e.,  $[H, \mathcal{RT}] = 0$ . As shown in Ref. [36], the effects of  $\mathcal{RT}$  symmetry are similar to that of  $\mathcal{PT}$  symmetry. In particular, the Hamiltonian always commutes with  $\mathcal{RT}$ , although  $H$  and  $\mathcal{RT}$  do not always share the same eigenvectors due to the antilinearity of  $\mathcal{T}$ , which leads to the parametric dependence having a real spectrum.

### A. Energy spectrum of $iATXY$ model

By performing Jordan-Wigner transformation followed by a Fourier transform of the fermionic operators, the  $iATXY$  model in Eq. (1) can be diagonalized by employing a procedure similar to the Hermitian  $ATXY$  model [40–42,46–48]. First, let us convert  $H_{iATXY}$  in terms of  $\sigma^+$  and  $\sigma^-$  operators, where  $\sigma^x = \frac{\sigma^+ + \sigma^-}{2}$ ,  $\sigma^y = \frac{\sigma^+ - \sigma^-}{2i}$ , and  $\sigma^z = \sigma^+ \sigma^- - \frac{1}{2}$ .

The Jordan-Wigner transformation,

$$\hat{\sigma}_{2j}^+ = \hat{e}_{2j}^\dagger \exp \left( i\pi \sum_{l=1}^{j-1} \hat{e}_{2l}^\dagger \hat{e}_{2l} + i\pi \sum_{l=1}^j \hat{\delta}_{2l-1}^\dagger \hat{\delta}_{2l-1} \right),$$

$$\hat{\sigma}_{2j+1}^+ = \hat{\delta}_{2j+1}^\dagger \exp \left( i\pi \sum_{l=1}^j \hat{e}_{2l}^\dagger \hat{e}_{2l} + i\pi \sum_{l=0}^{j-1} \hat{\delta}_{2l+1}^\dagger \hat{\delta}_{2l+1} \right)$$

maps the system into a 1D two-component Fermi gas, where the even and odd sites correspond to fermions, following the fermionic commutation rules, governed by  $\hat{e}$  and  $\hat{\delta}$ , respectively.

The parity operator, defined as  $\xi = \prod_{i=1}^N (\sigma_i^z) = (-1)^{N_f}$ , where  $N_f = \sum_{i=1}^N \hat{\delta}_{2i-1}^\dagger \hat{\delta}_{2i-1} + \hat{e}_{2i}^\dagger \hat{e}_{2i}$ , commutes with the Hamiltonian, i.e.,  $[H, \xi] = 0$ , which is the sum of the number of fermions. Considering the parity and the Jordan-Wigner transformation, the Hamiltonian can be written as

$$\hat{H}_{iATXY} = \sum_{i=1}^{\frac{N}{2}-1} [\hat{\mathcal{X}}_i + \hat{\mathcal{Y}}_i + i\gamma(\hat{\mathcal{V}}_i + \hat{\mathcal{W}}_i)] + h_o \hat{\mathcal{M}}_i^o + h_e \hat{\mathcal{M}}_i^e - \mu(\hat{\mathcal{Y}}_{\frac{N}{2}} + i\gamma \hat{\mathcal{W}}_{\frac{N}{2}}), \quad (2)$$

where  $\hat{\mathcal{X}}_i = \hat{\delta}_{2i-1}^\dagger \hat{e}_{2i} + \text{H.c.}$ ,  $\hat{\mathcal{Y}}_i = \hat{e}_{2i} \hat{\delta}_{2i+1}^\dagger + \text{H.c.}$ ,  $\hat{\mathcal{V}}_i = \hat{\delta}_{2i-1}^\dagger \hat{e}_{2i}^\dagger + \text{H.c.}$ ,  $\hat{\mathcal{W}}_i = \hat{e}_{2i}^\dagger \hat{\delta}_{2i+1}^\dagger + \text{H.c.}$ , and the last term is for the boundary condition, with  $\mu$  being the eigenvalue of  $\xi$  with distinct values of  $\pm 1$ . Here the numbers of odd and even fermions are given by  $\hat{\mathcal{M}}_i^o = \hat{\delta}_{2i-1}^\dagger \hat{\delta}_{2i-1}$  with field  $\lambda_o = 2(h_1 - h_2)/J$  and  $\hat{\mathcal{M}}_i^e = \hat{e}_{2i}^\dagger \hat{e}_{2i}$  with field  $\lambda_e = 2(h_1 + h_2)/J$ . We set  $h_i/J = \lambda_i$ ,  $i = 1, 2$ . Using Fourier transformations, given by

$$\hat{\delta}_{2j+1}^\dagger = \sqrt{\frac{2}{N}} \sum_{p=-N/4}^{N/4} \exp [i(2j+1)\phi_p] \hat{\delta}_p^\dagger,$$

$$\hat{e}_{2j}^\dagger = \sqrt{\frac{2}{N}} \sum_{p=-N/4}^{N/4} \exp [i(2j)\phi_p] \hat{e}_p^\dagger, \quad (3)$$

we write the Hamiltonian including the boundary terms, i.e., the summation of  $\sum_{i=1}^{\frac{N}{2}}$ , which can be done by considering suitable Fourier momenta: odd parity ( $\mu = -1$ ) is given by  $k^- = \frac{2\pi p}{N}$ , and even parity ( $\mu = +1$ ) is given by  $k^+ = \frac{2\pi(p+1/2)}{N}$ . The Hamiltonian can now be written in the Fourier basis,  $S^k = \{o_{k^\mu}, o_{-k^\mu}^\dagger, e_{k^\mu}, e_{-k^\mu}\}$ , as

$$H_{iATXY} = \sum_{k \in k^\mu} H_{iATXY}^k = \sum_{k \in k^\mu} (\hat{S}^k)^\dagger \hat{H}_{iATXY}^k \hat{S}^k. \quad (4)$$

Since the Hamiltonian is invariant under parity, the corresponding  $k^\pm$  do not mix, and hence, we can consider  $k$  to be a general momentum running through both even and odd momenta. Thus, the Hamiltonian  $H_{iATXY}^k$  reduces to

$$\begin{bmatrix} \lambda_1 + \cos k & -\gamma \sin k & 0 & -\lambda_2 \\ \gamma \sin k & -\lambda_1 - \cos k & \lambda_2 & 0 \\ 0 & \lambda_2 & \cos k - \lambda_1 & -\gamma \sin k \\ -\lambda_2 & 0 & \gamma \sin k & -\cos k + \lambda_1 \end{bmatrix}. \quad (5)$$

Diagonalizing  $H_{iATXY}^k$  gives the single-particle energy spectrum of the model in each  $k$  subspace in terms of  $\lambda_i$  ( $i = 1, 2$ ) and  $\gamma$  as

$$E_{\pm}^k = [\lambda_1^2 + \lambda_2^2 + \cos^2 k - \gamma^2 \sin^2 k \pm 2\sqrt{\lambda_1^2 \lambda_2^2 + h_1^2 \cos^2 k + \lambda_2^2 \gamma^2 \sin^2 k}]^{1/2}, \quad (6)$$

which finally leads to the energy spectrum of the model and hence can be used to obtain the exceptional points, dividing the regions of broken and unbroken phases in the  $iATXY$  model.

### III. BROKEN-UNBROKEN TRANSITION OF THE QUANTUM $iATXY$ MODEL AT THE FACTORIZATION SURFACE OF THE HERMITIAN MODEL

Having obtained the energy for each momentum space  $k$ , let us concentrate on the transition from the broken to unbroken phase. In other words, in the unbroken phase, the spectrum becomes real if the same set of eigenvectors spans both  $H$  and  $\mathcal{RT}$ , while in the broken phase, complex-conjugate pairs are the eigenvalues of  $\hat{H}_{iATXY}$ .

Let us identify the parameter space where the spectrum is real. To identify it, we will be looking for the value of  $k$  at which  $E_{\pm}^k$  has an extremum and  $(E_{\pm}^k)^2 \geq 0$ . It turns out that the value of  $k$  for which  $E_{\pm}^k$  reaches its extremum, i.e.,  $\frac{dE_{\pm}^k}{dk} = 0$ , is given by

$$k = \cos^{-1} \left( \sqrt{\frac{1}{\lambda_1^2 + \lambda_2^2 \gamma^2} \left[ \frac{\lambda_1^2 + \lambda_2^2 \gamma^2}{1 + \gamma^2} \right] + \lambda_2^2 \gamma^2 - \lambda_1^2 \lambda_2^2} \right). \quad (7)$$

Plugging it into  $E_{\pm}^k$  and checking when it is real, which is equivalent to finding out when  $(E_{\pm}^k)^2 \geq 0$ , we find that the

parameter space is split in order to have a real spectrum when

$$\begin{aligned} \lambda_1 &\geq \sqrt{1 + \lambda_2^2 + \gamma^2} \equiv \lambda_1^s, & \lambda_1 > \lambda_2, \\ \lambda_1 &\leq \sqrt{1 + \lambda_2^2 + \gamma^2}, & \lambda_1 < \lambda_2. \end{aligned} \quad (8)$$

Let us first note that the second case is not possible. The reason is that when  $\lambda_1 < \lambda_2$ , i.e., when  $\lambda_1^2 - \lambda_2^2 < 0$ , the real eigenvalues occur for  $\lambda_1^2 - \lambda_2^2 > 1 + \gamma^2$ , which is not possible since  $\gamma$  is real. Hence, the transition from the broken to unbroken phase happens when  $\lambda_1 \geq \sqrt{1 + \lambda_2^2 + \gamma^2}$ . Notice that for the uniform  $XY$  model, i.e., with  $\lambda_2 = 0$ , the eigenvalues go from real to complex pairs when  $\lambda_1 \geq \sqrt{1 + \gamma^2}$ , as found in Ref. [36]. Notice also that  $E_{\pm}^k$  does not lead to any useful condition in terms of  $\lambda_1, \lambda_2$ , and  $\gamma$ .

Apart from quantum critical points, the Hermitian  $ATXY$  model possesses a special point (surface) known as the factorization surface [14,40,42], denoted by  $\lambda_{1(H)}^f$ , which can be represented as

$$\lambda_{1(H)}^f = \sqrt{1 + \lambda_2^2 - \gamma^2} \quad (9)$$

in the parameter space. At this surface, the ground state is doubly degenerate and fully separable, having vanishing bipartite as well as multipartite entanglement.

If we now replace  $\gamma$  by  $i\gamma$  in Eq. (9), we recover the first condition of having a real spectrum in the  $iATXY$  model given in (8). We denote the right-hand side of (8) as  $\lambda_1^s$ . This suggests that the transition from the symmetry-broken phase to the unbroken phase of the  $\mathcal{RT}$ -symmetric Hamiltonian can be identified by the factorization surface of the corresponding Hermitian Hamiltonian.

Therefore, we propose the following: if the Hermitian Hamiltonian has a factorization surface  $\Lambda_{(H)}^f(\eta, \eta', \dots)$ , which is specified by the parameters of the Hamiltonian  $\eta, \eta', \dots$ , the corresponding  $\mathcal{RT}$ -symmetric Hamiltonian possesses real eigenvalues when  $\Lambda \geq \Lambda^s(i\eta, i\eta', \dots)$ , where some parameters can be complex to preserve the symmetry of the Hamiltonian.

Since the  $iATXY$  model can be solved analytically, we are able to derive the transition surface analytically. The above interesting observation can give us an important tool for detecting the phases of the non-Hermitian models, especially those models which cannot be solved analytically.

*Remark.* It is important to notice that the property obtained above is exclusive to the  $\mathcal{RT}$ -symmetric non-Hermitian system as opposed to the  $\mathcal{PT}$ -symmetric ones. For example, it was reported that a dimerized spin system with added imaginary local magnetic field with strength  $\eta$  conforms to  $\mathcal{PT}$  symmetry, having a real spectrum only when  $\eta < \eta_c$ , where  $\eta_c = \min[\text{sum of the interaction strengths in the } x \text{ and } y \text{ directions, difference of the interaction strengths in the } x \text{ and } y \text{ directions}]$  [31], which is not dictated by the factorization point [49].

In the rest of the paper, we demonstrate that the known factorization surface of the Hermitian model can, indeed, give the sufficient condition for the non-Hermitian nearest-neighbor  $iXYZ$  model with imaginary  $\gamma$ , as well as for the fully connected  $iATXY$  and the  $iXYZ$  models. Before addressing these models which cannot be solved analytically, we will now

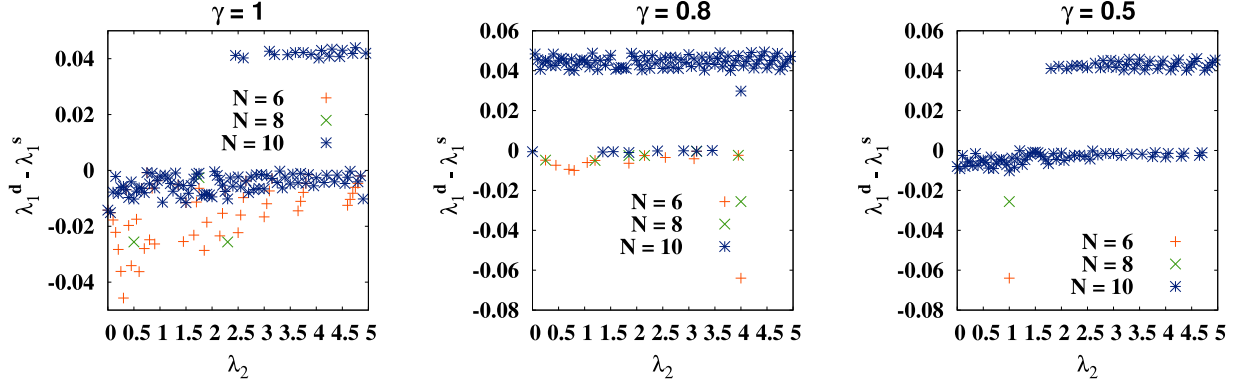


FIG. 1. Detected numerical value vs prediction of the  $iATXY$  model. The difference between the detected value,  $\lambda_1^d$ , found numerically (the value of  $\lambda_1$  at which the spectrum becomes real), and the predicted value,  $\lambda_1^s$  [according to (8)] (vertical axis), against  $\lambda_2$  (horizontal axis). The anisotropy of  $\hat{H}_{iATXY}$ ,  $\gamma$ , is fixed in each plot as shown at the top. The difference decreases with the increase in system size ( $N = 6, 8$ , and  $10$  are chosen to show convergence). Both axes are dimensionless.

check whether the condition for real eigenvalues in the  $iATXY$  model in (8) match the numerically obtained condition for real energies. Specifically, for a fixed  $N$ ,  $\lambda_2$ , and  $\gamma$ , we search numerically for  $\lambda_1$ , which gives the entire spectrum as real, and we match the detected value,  $\lambda_1^d$ , with  $\lambda_1^s$  obtained from condition (8).

We use the exact diagonalization technique which utilizes the Krylov subspace method, known as the Lanczos method [50]. Although it was noted [51] that the Arnoldi method may give better results for  $\mathcal{PT}$ -symmetric systems, we observe that there is no qualitative difference between the Lanczos and Arnoldi [52] methods. Both of these numerical mechanisms are part of ARMADILLO package [53,54], which we use to analyze our systems.

For a fixed anisotropy  $\gamma$ , Fig. 1 depicts the behavior of the difference,  $\lambda_1^d - \lambda_1^s$ , against  $\lambda_2$  from the  $iATXY$  model for different system sizes. Note that the numerical error is of the order of  $\pm 0.05$ , which is the same as the step size of  $\lambda_2$ . Figure 1 shows that our inference is in accordance with the numerical data under the specified numerical accuracy, which increases with the increase in the system size.

#### IV. CONNECTING THE FACTORIZATION POINT OF THE HERMITIAN MODEL WITH THE UNBROKEN PHASE OF $\mathcal{RT}$ -SYMMETRIC MODELS: SHORT- TO LONG-RANGE INTERACTIONS

In this section, we consider nearest-neighbor as well as long-range  $XYZ$  models with magnetic field with an imaginary anisotropy parameter and also long-range  $iATXY$  model. All these models have  $\mathcal{RT}$  symmetry, although they cannot be solved analytically. As mentioned before, we apply the exact diagonalization tool, mentioned in the previous section, to diagonalize the pseudo-Hermitian Hamiltonian and find the parameter space in which the eigenvalues are real.

##### A. $iXYZ$ model: Numerical versus prediction

Let us first consider the non-Hermitian nearest-neighbor  $XYZ$  Hamiltonian with  $\mathcal{RT}$  symmetry, which we call the

$iXYZ$  model, given by

$$\hat{H}_{iXYZ} = \sum_{i=1}^N J \left[ \frac{1+i\gamma}{4} \sigma_i^x \sigma_{i+1}^x + \frac{1-i\gamma}{4} \sigma_i^y \sigma_{i+1}^y + \frac{\tilde{\Delta}}{2} \sigma_i^z \sigma_{i+1}^z \right] + \frac{h}{2} \sigma_i^z, \quad (10)$$

where  $\tilde{\Delta}$  is the strength of the interaction in the  $z$  plane, and the other parameters are the same as in  $\hat{H}_{iATXY}$ . Here we set  $\Delta = \tilde{\Delta}/J$  and  $\lambda = h/J$ . It can be easy to find that  $[\hat{H}_{iXYZ}, \mathcal{RT}] = 0$ . Since we cannot diagonalize this Hamiltonian analytically, let us follow the prescription mentioned above to find the parametric condition for which the Hamiltonian has real eigenvalues. In this case, the factorization surface of the Hermitian  $XYZ$  model [15] is known to be

$$\lambda_{(H)}^f = \sqrt{(1+\Delta)^2 - \gamma^2}. \quad (11)$$

We propose that the spectrum becomes real when the magnetic field satisfies the condition given by

$$\lambda \geq \lambda^s \equiv \sqrt{(1+\Delta)^2 + \gamma^2}. \quad (12)$$

For a given  $\gamma$  and  $\Delta$ , we numerically find the actual  $\lambda^d$  for which all eigenvalues are real. In Fig. 2, for three different values of  $\gamma$ , the difference between the detected magnetic value  $\lambda^d$  and the predicted value  $\lambda^s$ , according to (12), is plotted. We observe that with the increase of  $N$ ,  $(\lambda^d - \lambda^s)$  are of the order of  $\pm 0.05$ , where the step size of  $\Delta$  is also considered to be 0.05. As shown in the case of the  $iATXY$  model, we can also report here that the prediction and numerical values are in good agreement, thereby verifying the prescription proposed to find the reality of the spectrum.

##### B. Pseudo-Hermitian model with long-range interactions

Up to now, all the spin models that we have discussed have nearest-neighbor interactions, and we showed that the unbroken-to-broken transition can faithfully be detected via the factorization surface of the respective Hermitian model. Let us now move to  $iATXY$  as well as  $iXYZ$  models with long-range interactions and show whether the sufficient condition for identifying the reality of the spectrum still remains

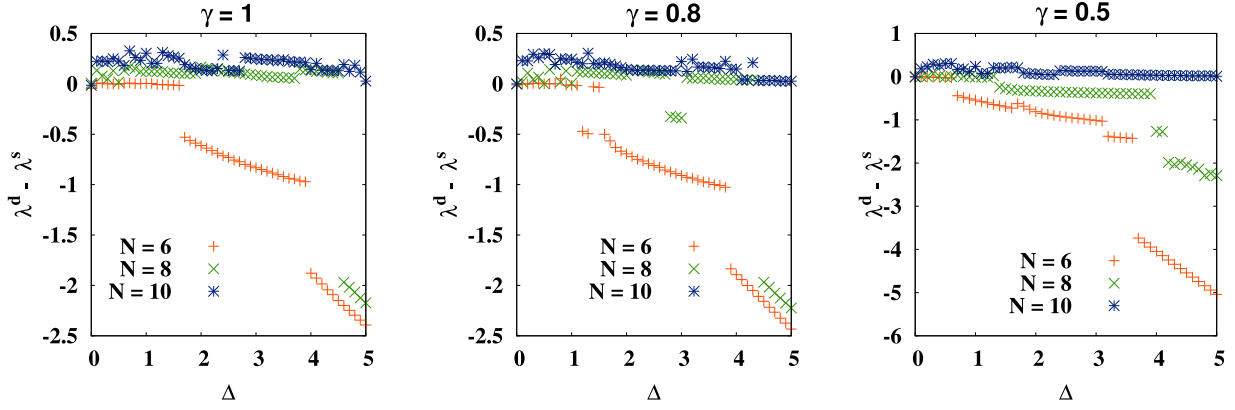


FIG. 2. Plot of  $\lambda^d - \lambda^s$  (vertical axis) vs  $\Delta$  (horizontal axis) of the  $iXYZ$  Hamiltonian  $H_{iXYZ}$ . An analysis similar to that in Fig. 1 is performed for the  $iXYZ$  model. Notice that for small system size  $N$ , the numerical values substantially differ from the inferred values for large  $\Delta$ . All other specifications are the same as in Fig. 1.

valid or not. It is important to note here that the long-range models are more likely to occur in experiments [55–61] and restricting interactions to just nearest neighbors is a tedious task in laboratories. Hence, a more experiment-friendly model is one in which the strength of the interactions decreases as the distance between the neighbors increases. We now carry out our analysis with this kind of model with  $\mathcal{RT}$  symmetry. In order to build the long-range model with  $\mathcal{RT}$  symmetry, we realize that other than the strength of the anisotropy involved in the interactions in the  $xy$  plane, we should not add imaginary terms in  $\Delta$  or  $\lambda_2$  since they fail to keep the symmetry.

### 1. $iATXY$ model with long-range interactions

Consider the  $iATXY$  model with long-range interactions, given by

$$\hat{H}_{iATXY}^L = \sum_{i=1}^N \sum_{j=i+1}^{i+\frac{N}{2}} J_{ij} \left[ \frac{1+i\gamma}{4} \sigma_i^x \sigma_j^x + \frac{1-i\gamma}{4} \sigma_i^y \sigma_j^y \right] + \frac{h_1 + (-1)^i h_2}{2} \sigma_i^z, \quad (13)$$

where the parameters except  $J_{ij}$  have the same features as in  $H_{iATXY}$  in Eq. (1). Here we consider power-law interactions, i.e.,  $J_{ij} = \frac{1}{|i-j|^\alpha}$ , where  $\alpha$  dictates how fast the interaction falls off with distance. For example, a very high  $\alpha$  value essentially imitates a nearest-neighbor model, while a low value corresponds to the situation when all of the spins interact with every other spin.

In this case, the factorization surface [17,18,62] is given as

$$\lambda_{1(H)}^f(\alpha) = \sqrt{1 + \lambda_2^2 - \gamma^2} \sum_{j=i+1}^{i+\frac{N}{2}} \frac{1}{|i-j|^\alpha}, \quad (14)$$

and hence, according to our recipe, the spectrum of  $\hat{H}_{iATXY}^L$  is real when

$$\lambda_1^\alpha \geq \lambda_1^s(\alpha) \equiv \sqrt{1 + \lambda_2^2 + \gamma^2} \sum_{j=i+1}^{i+\frac{N}{2}} \frac{1}{|i-j|^\alpha}. \quad (15)$$

By performing exact diagonalization of  $\hat{H}_{iATXY}^L$  for different system sizes, we uncover that for a fixed  $\lambda_2^\alpha$ , the difference between our prediction and the value of  $\lambda_1^\alpha$  at which the entire spectrum becomes real is not exactly zero. The reason behind such an observation is that the spectrum starts becoming real for some range of  $\lambda_1^\alpha$  and then again becomes imaginary, thereby creating a difficult situation for finding the exact transition point. However, when we start looking at and above  $\lambda_1^s(\alpha = 1)$ , we find that the eigenvalues always remain real. To ensure that this is true, in steps of 0.05, we check from the predicted  $\lambda_1^s(\alpha = 1)$  to  $\lambda_1^s(\alpha = 1) + 5.0$  and confirm that at all 100 points, the spectrum is real for a given  $\lambda_2^\alpha$ . Thus, as prescribed,  $\lambda_{1(H)}^f(\alpha)$  of the Hermitian model can suitably predict  $\lambda_1^s$ , which provides a sufficient condition for the unbroken phase of the pseudo-Hermitian model.

### 2. Long-range $iXYZ$ model:

#### Sufficient condition for the unbroken phase

Let us now analyze the  $\mathcal{RT}$ -symmetric  $iXYZ$  model when it is fully connected according to the power-law decay, represented as

$$\hat{H}_{iXYZ}^L = \sum_{i=1}^N \sum_{j=i+1}^{i+\frac{N}{2}} J_{ij} \left[ \frac{1+i\gamma}{4} \sigma_i^x \sigma_j^x + \frac{1-i\gamma}{4} \sigma_i^y \sigma_j^y + \frac{\tilde{\Delta}}{2} \sigma_i^z \sigma_j^z \right] + \frac{h}{2} \sigma_i^z, \quad (16)$$

where  $J_{ij}$  behave similarly as in Eq. (13). The factorization surface of the corresponding Hermitian model reads

$$\lambda_{(H)}^f(\alpha) = \sqrt{(1 + \Delta)^2 - \gamma^2} \sum_{j=i+1}^{i+\frac{N}{2}} \frac{1}{|i-j|^\alpha}, \quad (17)$$

which suggests that the point at which the eigenvalues of  $\hat{H}_{iXYZ}^L$  become real is

$$\lambda(\alpha) \geq \lambda^s(\alpha) = \sqrt{(1 + \Delta)^2 + \gamma^2} \sum_{j=i+1}^{i+\frac{N}{2}} \frac{1}{|i-j|^\alpha}. \quad (18)$$

Like in the long-range  $iATXY$  model, for a given  $\Delta$ , the  $\lambda(\alpha)$  at which the spectrum becomes completely real is hard

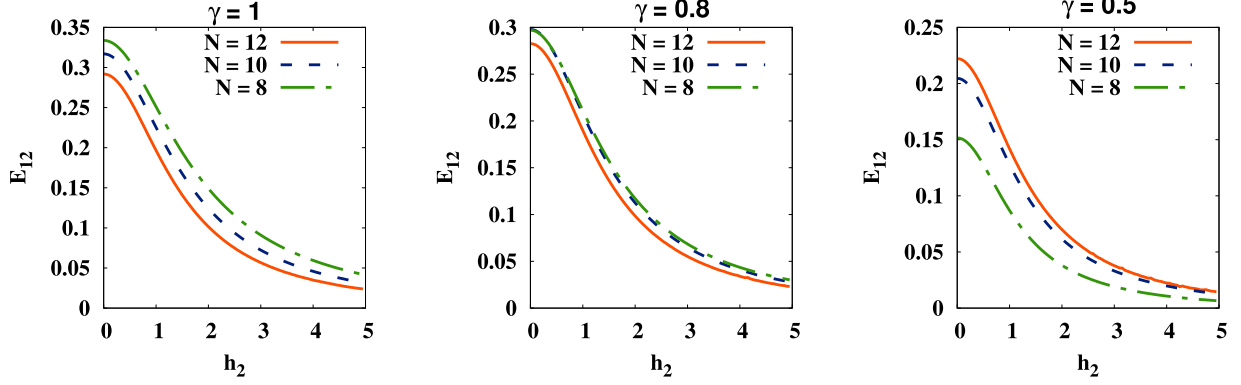


FIG. 3. Nearest-neighbor entanglement  $E_{12}$  (ordinate) of the zero-temperature state of the  $iATXY$  model at the exceptional point against  $\lambda_2$  (abscissa) for different system sizes. Here  $N = 8$  (long- and short-dashed lines),  $N = 10$  (dashed lines), and  $N = 12$  (solid lines). For given  $\gamma$  and  $\lambda_2$  values,  $\lambda_1^s$  is obtained via the condition (8). After tracing out every spin except the first and second, we find  $\rho_{12}$  and compute the bipartite entanglement measured by the logarithmic negativity  $E_{12}$  [63,64]. Both axes are dimensionless.

to find numerically. However, we apply the same method as before; i.e., with  $\Delta$  and varying  $\lambda(\alpha)$ , with  $\alpha = 1$ , in the range  $[\lambda^s(\alpha), \lambda^s(\alpha) + 5.0]$ , we observe that the eigenenergies are always real in that range, thereby confirming the sufficient condition for detecting the unbroken phase.

## V. BIPARTITE ENTANGLEMENT AND PARITY OF THE ZERO-TEMPERATURE STATE: NON-HERMITIAN AND HERMITIAN SYSTEMS

In this section, we compare the properties of the ground state for the  $\mathcal{RT}$ -symmetric and corresponding Hermitian systems. We calculate the parity and nearest-neighbor bipartite entanglement. Although the former feature indicates similarities between these two systems, the entanglement shows the opposite.

### A. Bipartite entanglement

We know that the factorization point in the Hermitian systems corresponds to a completely factorized ground state of

the form  $|\psi_1\rangle \otimes |\psi_2\rangle \dots \otimes |\psi_N\rangle$  with vanishing entanglement in all bipartitions. Let us examine the trends of entanglement at the surface where the broken-to-unbroken transition occurs in the  $iATXY$  model. In particular, we find that when we replace  $\gamma$  by  $i\gamma$ , the exceptional point  $\lambda_1^s$  is, indeed, not a factorization surface.

We observe that the nearest-neighbor entanglement  $E_{12}$  of the reduced bipartite state obtained from the zero-temperature state is nonvanishing at the exceptional surface given in (8), as depicted in Fig. 3. Notice that due to the translational symmetry of the model, all two-party nearest-neighbor states are the same, and hence, we calculate the logarithmic negativity [63,64] of  $\rho_{12}$  which is obtained after tracing out all the parties except the first and the second parties. We also find that the ground state is degenerate, and hence, we compute the bipartite entanglement of the canonical equilibrium state,  $\rho^\beta = e^{-\beta H_{iATXY}} / \text{Tr}(e^{-\beta H_{iATXY}})$ , with a very high  $\beta = 1/K_B T = 200$ ,  $T$  being the temperature and  $k_B$  being the Boltzmann constant. We call it the zero-temperature state.

It can be explained by considering a general two-site density matrix between spins  $a$  and  $b$ , which can be described in Pauli basis  $\sigma^{i=x,y,z}$  as

$$\rho_{ab}(m_i, m'_i, C_{ij}) = \frac{1}{4} \left( I_4 + \sum_{i=x,y,z} \left[ m_i(\sigma^i \otimes I_2) + m'_i(I_2 \otimes \sigma^i) + C_{ii}(\sigma^i \otimes \sigma^i) + \sum_{i \neq j=x,y,z} C_{ij}(\sigma^i \otimes \sigma^j) \right] \right),$$

where  $m_i = \text{Tr}(\rho_{ij}\sigma^i)$  and  $C_{ij} = \text{Tr}(\rho_{ij}\sigma^i \otimes \sigma^j)$ . The matrix form of  $\rho_{ab}$  can be written as

$$\rho_{ab} = \frac{1}{4} \begin{pmatrix} 1 + C_{zz} + m_z + m'_z & C_{zx} + m_x - im_y & m'_x - im'_y - iC_{yz} & C_{xx} - iC_{xy} - C_{yy} \\ C_{zx} + m_x + im_y & 1 - C_{zz} - m_z + m'_z & C_{xx} + iC_{xy} + C_{yy} & m'_x - im'_y + iC_{yz} \\ m'_x + im'_y + iC_{yz} & C_{xx} - iC_{xy} + C_{yy} & 1 - C_{zz} + m_z - m'_z & -C_{zx} + m_x - im_y \\ C_{xx} + iC_{xy} - C_{yy} & m'_x + im'_y - iC_{yz} & -C_{zx} + m_x + im_y & 1 + C_{zz} - m_z - m'_z \end{pmatrix}.$$

After taking the partial transposition over party  $b$ , the matrix looks like

$$\rho_{ab}^{T_b} = \frac{1}{4} \begin{pmatrix} 1 + C_{zz} + m_z + m'_z & C_{zx} + m_x + im_y & m'_x - im'_y - iC_{yz} & C_{xx} + iC_{xy} + C_{yy} \\ C_{zx} + m_x - im_y & 1 - C_{zz} - m_z + m'_z & C_{xx} - iC_{xy} - C_{yy} & m'_x - im'_y + iC_{yz} \\ m'_x + im'_y + iC_{yz} & C_{xx} + iC_{xy} - C_{yy} & 1 - C_{zz} + m_z - m'_z & -C_{zx} + m_x + im_y \\ C_{xx} - iC_{xy} + C_{yy} & m'_x + im'_y - iC_{yz} & -C_{zx} + m_x - im_y & 1 + C_{zz} - m_z - m'_z \end{pmatrix}.$$

From the above form, it is clear that  $\rho_{ab} = \rho_{ab}^{T_b}$  when  $\{m_y, C_{xy}, C_{yy}\} = 0$ , and hence, entanglement is vanishing. In the case of the Hermitian system, since the Hamiltonian is real, the ground state should contain only real numbers, which leads to  $\{m_y, C_{xy}\}$  being vanishing. Moreover, at the factorization point,  $C_{yy}$  also vanishes for the ground state. On the other hand, in the case of the  $\mathcal{RT}$ -symmetric Hamiltonian, which contains imaginary terms,  $\{m_y, C_{xy}, C_{yy}\} \neq 0$  for the ground state at the exceptional point. This leads to a nonvanishing entanglement even at the exceptional point. The results possibly indicate that introducing  $\mathcal{RT}$  symmetry in the system is another way to generate entanglement in the factorization surfaces (cf. [14]).

### B. Parity

As defined above, the parity operator  $\xi$  commutes with both the Hermitian and non-Hermitian Hamiltonians, i.e.,  $[\xi, H] = 0$ . It leads to their eigenstates having a definite parity,  $\mu = \pm 1$ . In the case of the Hermitian system, the parity of the ground state changes from negative to positive at the factorization point. A similar change in parity occurs for the  $\mathcal{RT}$ -symmetric Hamiltonian at the exceptional point.

## VI. CONCLUSION

We found that the factorization points of Hermitian quantum spin models dictate the exceptional points for the corresponding  $\mathcal{RT}$ -symmetric non-Hermitian Hamiltonians. As a demonstration, we analytically proved that the exceptional points of the non-Hermitian  $XY$  model with uniform and alternating transverse magnetic fields (the  $iATXY$  model) match the expression for the factorization surface of the nearest-neighbor  $ATXY$  model when the anisotropy parameter of the  $ATXY$  model is replaced by the imaginary one. Following this prescription, we were able to predict and nu-

merically verify the exceptional points of the nearest-neighbor  $iXYZ$  model. The other possible  $\mathcal{RT}$ -symmetric models considered here are long-range models, whose exceptional points are hard to find numerically. Hence, we provided a sufficient condition for obtaining the real energy spectrum using the factorization surface of the corresponding Hermitian model. Specifically, we observed that as long as the parameters of the non-Hermitian long-range  $iATXY$  and  $iXYZ$  models are above the factorization surfaces, the energy spectra are always real. Moreover, at the exceptional points, we computed the bipartite entanglement of the nearest-neighbor two-site reduced state obtained from the ground state and showed that it is nonvanishing, although entanglement vanishes at the factorization surface of the Hermitian counterpart.

Quantum spin models with higher-dimensional lattices as well as with long-range interactions can be studied only by using approximate methods or by numerical techniques. On the other hand, finding real or complex eigenvalues of the non-Hermitian spin models requires careful analysis of the entire energy spectrum, which is a difficult numerical task, as also mentioned in Ref. [51]. Therefore, the method proposed here to uncover the unbroken phase of the non-Hermitian models could be a useful mechanism to bypass the extensive numerical search.

## ACKNOWLEDGMENTS

We thank S. Mal for useful discussions. We also acknowledge the support from the Interdisciplinary Cyber Physical Systems (ICPS) program of the Department of Science and Technology (DST), India, Grant No. DST/ICPS/QuST/Theme- 1/2019/23. The authors acknowledge computations performed at the cluster computing facility of the Harish-Chandra Research Institute, Allahabad, India. Some numerical results were obtained using the Quantum Information and Computation library (QIClib).

- 
- [1] S. Sachdev, *Quantum Phase Transitions* (Cambridge University Press, Cambridge, 2009).
  - [2] B. K. Chakrabarti, A. Dutta, and P. Sen, *Quantum Ising Phases and Transitions in Transverse Ising Models* (Springer, Berlin, 1996).
  - [3] F. Verstraete and J. I. Cirac, *J. Stat. Mech.* (2005) P09012.
  - [4] T. Verkholyak, J. Strečka, F. Mila, and K. P. Schmidt, *Phys. Rev. B* **90**, 134413 (2014).
  - [5] M. Lewenstein, A. Sanpera, V. Ahufinger, B. Damski, A. Sen(De), and U. Sen, *Adv. Phys.* **56**, 243 (2007).
  - [6] I. Oliveira, R. Sarthour, Jr., T. Bonagamba, E. Azevedo, and J. C. Freitas, *NMR Quantum Information Processing* (Elsevier, Amsterdam, The Netherlands, 2011).
  - [7] K. R. K. Rao, H. Katiyar, T. S. Mahesh, A. Sen (De), U. Sen, and A. Kumar, *Phys. Rev. A* **88**, 022312 (2013).
  - [8] J. Zhang, M.-H. Yung, R. Laflamme, A. Aspuru-Guzik, and J. Q. Baugh, *Nat. Commun.* **3**, 880 (2012).
  - [9] R. Blatt and C. F. Roos, *Nat. Phys.* **8**, 277 (2012).
  - [10] R. Raussendorf and H. J. Briegel, *Phys. Rev. Lett.* **86**, 5188 (2001).
  - [11] R. Raussendorf, D. E. Browne, and H. J. Briegel, *Phys. Rev. A* **68**, 022312 (2003).
  - [12] P. Walther, K. J. Resch, T. Rudolph, E. Schenck, H. Weinfurter, V. Vedral, M. Aspelmeyer, and A. Zeilinger, *Nature (London)* **434**, 169 (2005).
  - [13] F. Campaioli, F. A. Pollock, and S. Vinjanampathy, *Thermodynamics in the Quantum Regime: Fundamental Aspects and New Directions*, edited by F. Binder, A. L. Correa, C. Gogolin, J. Anders, and G. Adesso (Springer International Publishing, Cham, 2018), pp. 207–225.
  - [14] T. Chanda, T. Das, D. Sadhukhan, A. K. Pal, A. Sen(De), and U. Sen, *Phys. Rev. A* **97**, 012316 (2018).
  - [15] J. Kurmann, H. Thomas, and G. Müller, *Physica A (Amsterdam, Neth.)* **112**, 235 (1982).
  - [16] S. M. Giampaolo, G. Adesso, and F. Illuminati, *Phys. Rev. B* **79**, 224434 (2009).
  - [17] N. Canosa, R. Rossignoli, and J. M. Matera, *Phys. Rev. B* **81**, 054415 (2010).
  - [18] M. Rezai, A. Langari, and J. Abouie, *Phys. Rev. B* **81**, 060401(R) (2010).

- [19] R. Rossignoli, N. Canosa, and J. M. Matera, *Phys. Rev. A* **77**, 052322 (2008).
- [20] R. Rossignoli, N. Canosa, and J. M. Matera, *Phys. Rev. A* **80**, 062325 (2009).
- [21] R. Horodecki, P. Horodecki, M. Horodecki, and K. Horodecki, *Rev. Mod. Phys.* **81**, 865 (2009).
- [22] C. M. Bender and S. Boettcher, *Phys. Rev. Lett.* **80**, 5243 (1998).
- [23] C. E. Rüter, K. G. Makris, R. El-Ganainy, D. N. Christodoulides, M. Segev, and D. Kip, *Nat. Phys.* **6**, 192 (2010).
- [24] G. Barontini, R. Labouvie, F. Stubenrauch, A. Vogler, V. Guarrera, and H. Ott, *Phys. Rev. Lett.* **110**, 035302 (2013).
- [25] C. Dembowski, H.-D. Gräf, H. L. Harney, A. Heine, W. D. Heiss, H. Rehfeld, and A. Richter, *Phys. Rev. Lett.* **86**, 787 (2001).
- [26] Y. Choi, S. Kang, S. Lim, W. Kim, J.-R. Kim, J.-H. Lee, and K. An, *Phys. Rev. Lett.* **104**, 153601 (2010).
- [27] L. Jin and Z. Song, *Phys. Rev. A* **80**, 052107 (2009).
- [28] Y. N. Joglekar, D. Scott, M. Babbey, and A. Saxena, *Phys. Rev. A* **82**, 030103(R) (2010).
- [29] L. Jin and Z. Song, *Phys. Rev. A* **81**, 032109 (2010).
- [30] O. Bendix, R. Fleischmann, T. Kottos, and B. Shapiro, *Phys. Rev. Lett.* **103**, 030402 (2009).
- [31] G. L. Giorgi, *Phys. Rev. B* **82**, 052404 (2010).
- [32] X. Z. Zhang, L. Jin, and Z. Song, *Phys. Rev. A* **85**, 012106 (2012).
- [33] L. Jin and Z. Song, *Phys. Rev. A* **84**, 042116 (2011).
- [34] L. Jin and Z. Song, *Ann. Phys. (NY)* **330**, 142 (2013).
- [35] L. Jin and Z. Song, *Phys. Rev. A* **85**, 012111 (2012).
- [36] X. Z. Zhang and Z. Song, *Phys. Rev. A* **87**, 012114 (2013).
- [37] E. Lange, G. Chimczak, A. Kowalewska-Kudłaszuk, and K. Bartkiewicz, *Sci. Rep.* **10**, 19906 (2020).
- [38] X. Z. Zhang and Z. Song, *Phys. Rev. A* **88**, 042108 (2013).
- [39] T. E. Lee, F. Reiter, and N. Moiseyev, *Phys. Rev. Lett.* **113**, 250401 (2014).
- [40] T. Chanda, T. Das, D. Sadhukhan, A. K. Pal, A. Sen(De), and U. Sen, *Phys. Rev. A* **94**, 042310 (2016).
- [41] U. Divakaran, A. Dutta, and D. Sen, *Phys. Rev. B* **78**, 144301 (2008).
- [42] S. Roy, T. Chanda, T. Das, D. Sadhukhan, A. Sen(De), and U. Sen, *Phys. Rev. B* **99**, 064422 (2019).
- [43] E. Lieb, T. Schultz, and D. Mattis, *Ann. Phys. (NY)* **16**, 407 (1961).
- [44] P. Jordan and E. P. Wigner, in *The Collected Works of Eugene Paul Wigner* (Springer, Berlin, Heidelberg, 1993), pp. 109–129.
- [45] P. Pfeuty, *Ann. Phys. (NY)* **57**, 79 (1970).
- [46] S. Deng, G. Ortiz, and L. Viola, *Europhys. Lett.* **84**, 67008 (2009).
- [47] J. Perk, H. Capel, M. Zuilhof, and T. Siskens, *Physica A (Amsterdam, Neth.)* **81**, 319 (1975).
- [48] K. Okamoto and K. Yasumura, *J. Phys. Soc. Jpn.* **59**, 993 (1990).
- [49] G. L. Giorgi, *Phys. Rev. B* **79**, 060405(R) (2009).
- [50] C. Lanczos, *J. Res. Natl. Bur. Stand.* **45**, 255 (1950).
- [51] C. M. Bender and D. J. Weir, *J. Phys. A* **45**, 425303 (2012).
- [52] W. E. Arnoldi, *Q. Appl. Math.* **9**, 17 (1951).
- [53] C. Sanderson and R. Curtin, *J. Open Source Software* **1**, 26 (2016).
- [54] C. Sanderson and R. Curtin, in *International Congress on Mathematical Software* (Springer, Cham, 2018), pp. 422–430.
- [55] M. Saffman, T. G. Walker, and K. Mølmer, *Rev. Mod. Phys.* **82**, 2313 (2010).
- [56] B. Neyenhuis, J. Zhang, P. W. Hess, J. Smith, A. C. Lee, P. Richerme, Z.-X. Gong, A. V. Gorshkov, and C. Monroe, *Sci. Adv.* **3**, 1700672 (2017).
- [57] R. Islam, C. Senko, W. C. Campbell, S. Korenblit, J. Smith, A. Lee, E. E. Edwards, C.-C. J. Wang, J. K. Freericks, and C. Monroe, *Science* **340**, 583 (2013).
- [58] M. Tezuka, A. M. García-García, and M. A. Cazalilla, *Phys. Rev. A* **90**, 053618 (2014).
- [59] A. M. Lobos, M. Tezuka, and A. M. García-García, *Phys. Rev. B* **88**, 134506 (2013).
- [60] T. Lahaye, C. Menotti, L. Santos, M. Lewenstein, and T. Pfau, *Rep. Prog. Phys.* **72**, 126401 (2009).
- [61] P. Jurcevic, B. P. Lanyon, P. Hauke, C. Hempel, P. Zoller, R. Blatt, and C. F. Roos, *Nature (London)* **511**, 202 (2014).
- [62] J. Abouie, M. Rezai, and A. Langari, *Prog. Theor. Phys.* **127**, 315 (2012).
- [63] G. Vidal and R. F. Werner, *Phys. Rev. A* **65**, 032314 (2002).
- [64] Entanglement of a bipartite state  $\rho_{ij}$  can be measured by logarithmic negativity [63], which is defined as follows:  $E(\rho_{ij}) = \log_2[2\mathcal{N}(\rho_{ij}) + 1]$ , where  $\mathcal{N}$  quantifies the sum of the absolute values of all the negative eigenvalues of a partially transposed matrix, denoted by  $\rho_{ij}^T$ .